What about limb long bone nutrient canal(s)? - A 3D investigation in mammals

A. Houssaye, Jocerand Prévoteau

1 **What about limb long bone nutrient canal(s)? – A 3D investigation in**
2 **mammals**

3

4 Alexandra Houssaye[1],* and Jocerand Prévoteau[1]

5 *[1]UMR 7179 CNRS/Muséum national d'Histoire naturelle, Département Adaptations du vivant,*
6 *57 rue Cuvier CP-55, 75005 Paris, France.*

7

8 RH: Mammal limb long bone nutrient canals

9

10

11

12

13

14

15

16

17

18

19

20

21

22 * Corresponding author

23 houssaye@mnhn.fr

24 Tel: +33140794866

25

Abstract

26

27 The nutrient arteries, located in the long bone diaphysis, are the major blood supply to long

28 bones, especially during the early phases of growth and ossification. Their intersection with

29 the central axis of the medullary area corresponds to the ossification center, and their opening

30 on the outer bone surface to the nutrient foramen. Nutrient arteries/foramen have essentially

31 been analyzed in humans, and only to a much lesser extent in a few mammals. Some studies

32 have taken measurements of the nutrient foramen; others have investigated the shape and

33 orientation of the nutrient canals but only partially. No studies have analyzed the nutrient

34 canal in three dimensions inside the bone and the relationships between nutrient foramen,

35 nutrient canal, growth, and physiology require to be further investigated. The current study

36 proposes to investigate in three dimensions the shape of the nutrient canal in stylopod bones

37 of various mammals. It defines qualitative and quantitative parameters in order to discuss the

38 diversity in e.g., morphology, orientation, and diameter encountered, resorting to two different

39 datasets in order to maximize differences within mammals and then analyze variation within

40 morphologically and phylogenetically closer taxa. This study highlights a strong intraspecific

41 variation for various parameters, with limited biological signal, but also shows trends. It

42 notably evidences that canals are generally more numerous and relatively thinner in less

43 elongated bones. Moreover, it shows that the growth center is located distally in the humerus

44 and proximally in the femur and that the canals are essentially oriented towards the faster

45 growing end, so that the nutrient foramen does not indicate the location of the growth center.

46 This result seems general in mammals but cannot be generalized outside of Mammalia.

47 Further analyses of the features of nutrient arteries in reptiles are required in order to make

48 comparisons with the trends observed in mammals.

49

50 Key words: Bone growth; femur; growth center; humerus; Mammalia; nutrient artery; nutrient

51 foramen; shape

52

53

Introduction

Bone is a connective tissue whose matrix mineralizes. This hard tissue constitutes the
skeleton, which provides support and protection and enables locomotion. Bones can notably
be distinguished based on their position within the skeleton and their shape. Limb long bones
occur in the stylopod (e.g. femur) and zeugopod (e.g. tibia) regions of the limbs. They are
morphologically divided into a shaft bounded by both proximal and distal ends, called
epiphyses (with intermediate metaphyses). The diaphysis of long bones is often (but not
always) tubular, i.e. compact bone deposits surround an empty medullar cavity. Conversely,
epiphyses are generally spongy (Carter & Beaupré, 2007). Long bones form through two
distinct modes of ossification: periosteal, i.e., direct ossification in the periosteum (membrane
covering the outer surface of the bone), and endochondral, i.e. following the resorption of a
preformed cartilaginous structure (Ross & Pawlina, 2011). In long bones, after the formation
of a cartilage model, periosteal bone deposits laterally and centrifugally. The cartilage inside
the shaft starts calcifying and blood vessels invade the calcified cartilage. Then resorption
occurs and a primary center of ossification develops, from which endochondral ossification
starts proximally and distally centrifugally, with synchronous periosteal bone deposition
(laterally) (Carter & Beaupré, 2007). The development of secondary centers of ossification in
the epiphyses can develop, pending on the taxa (e.g. it occurs in mammals, lepidosaurs but not
in turtles and crocodiles; Haines, 1969).

Nutrient foramina are openings through which blood vessels and peripheral nerves
connect the marrow. If there can be epiphyseal and metaphyseal arteries, the nutrient arteries
are located in the long bone diaphysis. The nutrient arteries are the major blood supply to long
bones, especially during the early phases of growth and ossification (Gümüsburun et al.
1994). The ossification center is considered to correspond to the intersection of the nutrient
canal(s) with the central axis of the medullary area (Digby, 1916).

If growth can be fast symmetrical in the proximal and distal directions, and thus the
growth center localized around mid-shaft, asymmetrical proximo-distal growth has been
reported since the 18th Century (Ollier, 1867; Bisgard & Bisgard, 1935; Payton, 1932); it is
considered rather constant in position for a given bone (Pereira et al. 2011) or not (Campos et
al. 1987). Moreover several studies mentioned the occurrence of several nutrient canals
(Mysorekar, 1967; Sendemir & Cimen, 1991; Gümüsburun et al. 1994), or the absence of
nutrient canal (Longia et al. 1980); they did not see any significant relationship between this

87 number and the bone length or the number of ossification centers (Patake & Mysorekar,

88 1977). The number of nutrient canals seems to greatly vary intraspecifically for a given bone

89 (Sendemir & Çimen, 1991; Pereira et al. 2011).

90   The nutrient arteries are supposed to enter the bone through a discrete foramen, the

91 nutrient foramen, on the diaphysis. This nutrient is considered as originally indicating the

92 position of the growth center; however, when the shaft extends asymmetrically in length, it

93 becomes proximally or distally located relative to the growth center (Hughes, 1952).

94 Considering the possible occurrence of several nutrient foramina and the asymmetrical

95 proximo-distal growth, the relationship between nutrient foramen, nutrient canal, and growth

96 center requires to be further investigated.

97   Beyond knowledge about growth mode, the nutrient canals are also supposed to bear

98 physiological information. Some studies have indeed concluded that a greater blood pressure

99 engenders a thickening and strengthening of the walls, as well as an increase in the

100 circumference of vascular canals (Seymour et al. 2011). The nutrient canal could thus be

101 larger in taxa showing a higher metabolic rate.

102   Nutrient arteries/foramen have essentially been analyzed in humans, and only to a

103 much lesser extent in a few mammals (e.g., Ahn, 2013 on dogs). It has also been visualized in

104 a few turtles (Nakajima et al. 2014). Some studies have taken measurements of the nutrient

105 foramen (Seymour et al. 2011); others have investigated the shape and orientation of the

106 nutrient canals but only partially, for example using needles inserted through the nutrient

107 foramen to get insights into the diameter (considering the diameter of the largest needle that

108 could be inserted more than 1cm deep) and the orientation (penetration direction of the

109 needle; Sim & Ahn, 2014), but no study has analyzed the nutrient canal in three dimensions

110 inside the bone.

111   The current study proposes to investigate the shape of the nutrient canals in stylopod

112 bones of various mammals. It proposes the definition of qualitative and quantitative

113 parameters in order to discuss the diversity in morphology, orientation, diameter…

114 encountered, resorting to two different datasets in order to maximize differences within

115 mammals and then analyze these variations within morphologically and phylogenetically

116 closer taxa. This enables to discuss the growth mode of the stylopod bones in various

117 mammals, the biological signal of some features of the nutrient canals, and the degree of

118 interspecific and intraspecific variation observed.

119

120

4

Material and methods

Material

The material includes humeri and femora from two datasets (see Table 1) already available from previous studies (Houssaye et al. 2018; Houssaye & Botton-Divet, 2018), and representing adult specimens. The first one (hereafter referred to as QM) consists in 15 quadrupedal mammal species of various sizes, morphologies, locomotor modes, and they are widespread on mammal phylogeny (see Table 1). The aim of this sample is to show diversity, despite a limited sample size. The other sample (hereafter referred to as MU) is more restricted (in e.g., morphology, size and phylogenetic position). It focuses on mustelids, with 10 species (3 common with the previous sample) illustrating diverse degrees of adaptation to an aquatic lifestyle (terrestrial, semi-aquatic, aquatic).

Methods

Data acquisition

Bones were scanned using high-resolution computed tomography (GE_phoenix|X-ray v|tome|xs 240) at the Steinmann-Institut, University of Bonn (Germany) and at the AST-RX platform at the Museum national d'Histoire naturelle, Paris (France), with reconstructions performed using DATOX/RES software. Voxel size naturally varies pending on specimen size, from 19 to 246 μm. Image segmentation and visualization were performed from the reconstructed image data using Avizo 9.4 (VSG, Burlington, MA, USA).

The nutrient canals were segmented. The limits of the canals were difficult to clearly fix: at the outer surface, notably because of the obliquity of the canal; in the medullary area, because of bone resorption. Some canals were located more distally or proximally on the bone and not linked to the diaphyseal growth center; they thus appeared rather as metaphyseal or epiphyseal canals and were not taken into consideration.

Data analysis

The following parameters were defined in order to qualitatively and quantitatively characterize the nutrient canals: 1) number of nutrient canals in the bone (NNC); 2) mean diaphyseal radius (R), averaged for the whole diaphysis, based on the averaged sectional area

154   (averaged CSA parameter in BoneJ), as $\sqrt{(\text{averaged CSA}/\pi)}$; 3) the foraminal index (FI); this

155   index was defined by Hughes (1952) to estimate the relative position of the nutrient foramen

156   on the bone; it is calculated as the ratio of the distance between the proximal extremity of the

157   bone and the nutrient foramen (d) over the bone total length (Kizilkanat et al. 2007). Because

158   some epiphyses were incomplete (on the scans), the missing part was estimated based on

159   comparisons with similar bones (e.g., on archeozootheque;

160   https://www.archeozoo.org/archeozootheque/), and the points chosen to calculate the

161   distances do not correspond to the most extremes points: in the humerus, the proximal point

162   corresponds to the most distal point between the humeral head and the greater tubercle on the

163   proximal surface; the distal point corresponds to the core of the trochlea; in the femur, the

164   proximal point is the most distal point between the femoral head and the greater trochanter

165   and the distal point is located at the core of the patella groove (Fig. 1); 4) canal diameter (CD)

166   calculated based on the mid-canal sectional area (CA) obtained in Artec Studio Professional

167   v12.1.5.1 software (Artec 3D, 2018) with the measuring tool "section", as $\sqrt{(\text{CA}/\pi)}$. The

168   parameter is calculated at the mid-length of what is preserved (not resorbed) of the canal

169   walls, the section of the canal being usually rather constant except around its extremities; 5)

170   canal diameter at the outer extremity (CDE), in order to take into consideration the variation

171   of the canal diameter along its length, calculated as for CD but based on the most external

172   section perpendicular to the canal; 6) canal obliquity (CO); this parameter had previously

173   been analyzed based on the insertion of a needle in the canal and the measurement of the

174   angle between the needle and the long bone longitudinal axis (Sim & Ahn, 2014). Here since

175   we have access to the 3D organization of the canal and sometimes observe orientation

176   changes along the canal, we measured the general obliquity as the angle between a line

177   linking the canal extremities as preserved and the horizontal to the bone longitudinal axis; 7)

178   Canal cortical height (H) representing the relative height of the reconstructed canal (that could

179   essentially be reconstructed in the cortex) divided by the bone length as measured for FI.

180   Parameters linked to canal length (and thus also volume) could not be obtained because of

181   resorption occurring in the medullary area. Two additional parameters were defined in order

182   to estimate the bone length and shape: L- bone length, as measured for FI; and LR- bone

183   length (L) divided by the bone mean diaphyseal radius (R).

184   In addition to these quantitative parameters, some qualitative ones were also defined:

185   a) direction: proximal to distal (PD) or distal to proximal (DP); b) shape; it defines the global

186   shape of the canal: straight or angled; c) orientation: it describes the anatomical orientation of

187   the canal in the bone.

188

189   We tested the phylogenetic signal of the continuous parameters in the data. For that we

190   averaged the values obtained for all canals (when several canals occurred) and all specimens

191   (when several specimens were available) for each species. Then we calculated the K-statistic

192   following Blomberg *et al.* (2003) for each parameter and performed randomization tests. The

193   K-statistic compares the observed phylogenetic signal in a trait with the signal under a

194   Brownian motion model of trait evolution. A K-value > 1 implies more similarity between

195   relatives than expected under Brownian motion; K < 1 highlights convergences. We used the

196   phylogeny from Meredith et al. (2011) and from Slater et al. (2012) for the quadrupedal

197   mammal (QM) and mustelid (MU) samples, respectively (Fig. S1).

198   We tested the influence of size on all parameters, first on all canals independently,

199   then for each specimen, and thus grouping data for all canals for each specimen. In order to do

200   so, we averaged all parameters but also calculated the sum of the canal diameters: CDsum and

201   CDEsum. We performed linear regressions of each parameter to R.

202   In order to evaluate how these different parameters drive the variation observable in

203   our samples, we conducted normalized PCAs (David & Jacobs, 2014) for all datasets, those

204   with all canals and those averaged by specimen.

205   These analyses and additional statistical ones (Student's t-test, Anova) were performed

206   using statistical software R (R Core Team, 2014).

207

208

209   **Results**

210   The values obtained for the different parameters are listed in Tables S1-4.

211

212   **Discrete parameters**

213   *The number of nutrient canals (NNC)*

214   It varies from one to four in our samples. It varies among a single species (e.g. from 1 to 3 in

215   the humerus of *Mustela putorius*) and between humeri and femora from the same species (1 in

216   the humerus, 4 in the femur of *Erinaceus europaeus*). Correlation tests between the humerus

217   and femur datasets averaged for each species indicate no correlation between the two bones.

218   Anovas revealed that the number of canals is always correlated with LR, and thus the bone

219   proportions, and CDr (but not always with CDEr; Table 2). LR decreases when the bone is

220   more robust for a given length. In less elongated bones, canals appear generally more

221 numerous and relatively thinner. But, as shown by the intraspecific variation, this is a

222 common but not absolute trend.

223

224 *Direction*

225 Canals are mainly directed distalo-proximally (from the core to the outer surface of the bone)

226 in the humerus (Fig. 2A). There are a few exception, with proximo-distal orientations in

227 *Meles meles*, one specimen of *Mustela putorius*, *Pteronura brasiliensis* and *Lontra felina*, and

228 one of the two canals of the *Mustela eversmanni* specimen. From our sample, it thus only

229 varies from the common condition in mustelids. In addition, a few canals are sub-horizontal,

230 which usually corresponds to CO values lower than 15° (Fig. 2B). This occurs only in bones

231 with several canals (except in the specimen of *Lutra lutra*). Conversely, in the femur, canals

232 are mainly proximo-distally directed (Fig. 2C-D). Exceptions occur in *Rangifer tarandus*,

233 *Vulpes vulpes*, and one of the canals of *Erinaceus europaeus, Rupicapra rupicapra*, and

234 *Mustela eversmanni*. One horizontal canal is observed in one of the canals of *Choeropsis*

235 *liberiensis*.

236   Canals are essentially straight, except in *Rangifer*'s humerus and femur and in several

237 bones of mustelids where they are angled: the humerus of *Meles*, *Martes*, two *M. putorius*,

238 one canal of *M. eversmanni*, one canal of one *Enhydra lutris*. Moreover, a humerus of *Lontra*

239 *felina* shows a serpentiform canal. Conversely all canals in the mustelid femora are straight.

240

241 The orientation of the canals in the bone. It is extremely variable in the humeri and femora of

242 the QM sample; they can extend either anteriorly, posteriorly, medially, laterally or in

243 between. In the humerus of the mustelids, most canals are anteriorly directed, some medially

244 and a few posteriorly directed. No canal is laterally oriented. In the femora, canals are almost

245 always posteriorly oriented, only a few being medially oriented.

246

247 **Continuous parameters**

248 *Phylogenetic signal*

249 There is no phylogenetic signal in the parameters used to describe the canals for the QM

250 dataset (Table 3). However, within mustelids, a phylogenetic signal is observed in some

251 parameters (sometimes with a high K value) but not for the same parameters in the humerus

252 as in the femur, except for CDE (Table 3). There is a significant phylogenetic signal for the

253 size index R only for the Humerus QM (with no other parameter showing a significant

8

254 phylogenetic signal in this sample). The occurrence of a phylogenetic signal in the data

255 appears thus clearly independent of size.

256

257 *Influence of size*

258 Linear regressions clearly show that the canal diameter is correlated with size, whereas its

259 geometry is not, in all datasets (Table 4). For further analyses we used ratios for the canal

260 diameter parameters, dividing their values by R (CDr,CDEr, CDrsum, CDErsum).

261

262 *Values of the parameters*

263 The continuous parameters are discussed based on datasets considering all canals (Fig. 3). The

264 foraminal index (FI) is clearly higher in humeri than femora (t.tests; p<0.001; Fig. 3A). It is

265 also slightly lower in the QM sample than in the MU one (t.tests; p<0.001; Fig. 3A). For the

266 canal diameter parameters, no significant difference is observed between the various datasets

267 (Fig. 3B-C). The canal obliquity (CO) and the canal cortical height (H) are much higher in

268 otter femora (t.tests; p<0.001; Fig. 3D-E).

269

270 *Principal component analyses*

271 The PCAs enable not only to study the distribution of the different specimens in the

272 morphospace, but also and above all in our study, to analyze the relative contribution of each

273 parameter to the others and to compare results obtained based on the different datasets.

274

275 Quadrupedal mammals

276   The first two axes of the humerus PCA including all canals (representing 87.1% of the

277 total variance; Fig. 4) show that several canals from the same specimen can be either close (as

278 for *Talpa*; Te) or very distant (as for *Choeropsis*; Cl). The intrabone variation seems thus

279 potentially very high. In this small sample, the intraspecific variation seems essentially driven

280 by the canal geometry (H, CO, FI). About the variables, the two canal diameter parameters

281 co-vary. H and FI vary antagonistically. When data are averaged for each specimen, the

282 relationships between the variables remain similar.

283   The first two axes of the femur PCA including all canals (representing 78.6% of the

284 total variance; Fig. 5A) also show a strong covariation between the two canal diameter

285 parameters. The obliquity (CO) and canal cortical height (H) also strongly co-vary. As for the

286 humerus, the intrabone variation varies between taxa (rather weak in *Talpa* [Te], high in

287 *Erinaceus* [Ee] and *Rupicapra* [Rr]) and appears clearly affected by various parameters

288 pending on the specimens. Whereas CDr and CDEr rather co-vary with CDrsum and

289 CDErsum for the humerus when data are averaged for each specimen, this is not the case for

290 the femur, where the first ones drive variability essentially along the first axis and the others

291 along the second axis (Fig. 5B). The relationships between the variables are rather consistent

292 between the two femur PCAs, with the averaged CDr and CDEr replacing the CDr and CDEr

293 values. The addition of the CDrsum and CDErsum does not change much the relative

294 distribution of the specimens in the morphospace.

295 Mustelids

296   The first two axes of the PCA for all canals of the humeri (representing 82.3% of the

297 variance; Fig. 6A) clearly show that variation within a bone can be greater than between

298 specimens (e.g. in *Enhydra lutris* [El], *Lontra canadensis* [Lc]). In this taxonomically more

299 narrow sample, the relationships between the different variables is similar as in the QM

300 sample, with a slightly lower co-variation between CDr and CDEr. When data are grouped by

301 specimens, the CDEr and CDErsum variables separate from the CDr and CDrsum ones that

302 strongly co-vary (Fig. 6B). The distribution of the specimens in the morphospace is this time

303 different between the two samples (e.g. *Meles* [Mm]).

304   The first two axes of PCA for all canals of the femora (representing 90.7% of the

305 variance) tend to separate otters (lutrines) from other mustelids, with a limited overlap. H and

306 FI strongly co-vary, slightly less with CO, whereas, at about right angle to those variables,

307 CDr and CDEr also strongly co-vary. As for the humerus, variation within a bone can be

308 higher than between bones of a same species and even between species (Fig. 7). When canals

309 from single specimens are globally considered, all canal diameter variables co-vary and with

310 the same relationship to the other variables as CDr and CDEr in the previous analysis. The

311 distribution of the specimens is also similar.

312

313 Considering the divergence between lutrines and mustelines in the mustelid sample of femora

314 and based on the strong differences in femur shape and proportions between these two groups

315 (Botton-Divet et al. 2016), we analyzed the possible correlation between bone proportions and

316 the various parameters, assuming a possible link with the canal geometry parameters. For that

317 we performed linear regressions of all datasets with L and LR (Table 5).

318   These analyses reveal that there is no correlation between bone length (L) and the

319 canal parameters (only two significant results for distinct parameters and datasets), but also no

320 general correlation between bone proportions, i.e. notably between small and large bones

321 versus elongated ones, and the canal parameters. Indeed only CDr shows a significant link but

322 only for three of the four datasets. However, it is clear that the link is stronger for otter

323 femora, all parameters except CO showing a significant correlation with LR in both datasets.

324 The canal features (except CO) are thus strongly linked with the bone proportions in the

325 mustelid femora.

326   Correlation tests between the humerus and femur datasets averaged for each species

327 indicate a significant correlation for the canal diameter parameters but not for the others.

328

Discussion

330 Our study was the first one, to our knowledge, to analyze in three dimensions both

331 qualitatively and quantitatively the nutrient canals in limb bones thanks to the use of

332 microtomography. We proposed various parameters to describe their features, and analyzed

333 their values in two mammal samples in order to discuss their biological significance.

334

335 *General comparisons*

336 We did not observe a general phylogenetic signal in the quantitative parameters used to

337 describe the canals. Indeed, a phylogenetic signal was observed for some parameters in the

338 MU sample, but not for the same parameters in the two bones (except CDE). Moreover, no

339 parameter was showing a significant phylogenetic signal in the QM sample. The occurrence

340 of a phylogenetic signal seems thus very dependent on the sample.

341

342 In all our analyses, intraspecific variation and even intrabone variation was often very high

343 and sometimes much higher than interspecific variation. As a consequence, the nutrient canals

344 appear to be poor indicators of biological features of a taxon or even organism. Nevertheless,

345 some specific features could be identified, like the correlation between the canal features and

346 the bone proportions in the MU femora (and not in other samples) notably distinguishing

347 between otters and mustelines. This raises the potential interest in analyzing in detail the

348 biological signal of nutrient foramina in taxonomically smaller taxa. The parameters CD and

349 CDE were co-varying in all analyses, so that we would suggest the use of only one of these

350 parameters in further studies. The other parameters analyzed appear suitable to describe the

351 diversity of the canal shape.

352

353 *Number and diameter of the nutrient canals*

11

354   This study showed in limb bones a number of nutrient canals varying from one to four, but

355   more generally between one and two, in its samples. Previous studies on human long bones

356   described a majority of humeri with a single nutrient foramen and of femora with one or two

357   nutrient foramina, some also showed up to nine et even no foramen at all (Longia et al. 1980;

358   Sendemir & Cimen, 1991; Nagel, 1993; Gümüsburun et al. 1994; Kizilkanat et al. 2007).

359   During our study, we could observe that some metaphyseal canals exit the bone in the

360   diaphysis, so that some nutrient foramina on the diaphysis can belong to metaphyseal rather

361   than diaphyseal nutrient canals.

362   In our samples, the number of canals varies also within a single species (e.g. from 1 to

363   3 in the humerus of *Mustela putorius*) and between humeri and femora from the same species.

364   This parameter appears thus strongly variable intraspecifically. However, our study reveals a

365   trend for nutrient canals to be generally more numerous and relatively thinner in less

366   elongated bones. As for the canal diameter, the diameters taken at mid-length or at the

367   periphery co-vary. These parameters are also the only one to co-vary between the humeri and

368   the femora. This shows that the diameter of the canals is rather constrained. Seymour et al.

369   (2011) suggested a link between blood vessel circumference and metabolic rates (larger blood

370   vessels to service higher flow rates) and thus that the diameter of the nutrient canals would be

371   linked to the physiology of the organisms. Our results confirm that the size of the canals

372   appears constrained and rather homogeneous within a specimen.

373

374   *Canal direction and orientation*

375   In humeri, canals are essentially distalo-proximally directed, whereas it is the opposite in the

376   femur. However foraminal indices are much higher in humeri than in femora, in accordance

377   with studies on human bones (Pereire et al. 2011). It is because the growth center is located

378   much more distally in the humerus than in the femur (in our samples). The nutrient canal

379   seems thus generally oriented towards the mid-diaphysis. Unfortunately, because the

380   centralmost part of the bones generally underwent resorption, the medialmost extension of the

381   nutrient canals is not observable. As a consequence, the position of the growth center cannot

382   precisely be ascertained. If in the case of straight canals, it would be tempting to extend the

383   canal up to the core of the shaft, the occurrence of some bending in a few canals or of a slight

384   change of orientation close to the growth center (e.g. femur of *Enhydra*) prevents the use of

385   such an approach. When several canals occur, the intersection of the canals can also be

386   ascertained as the position of the growth center. Despite the difficulty in determining the exact

387   position of the growth center, the position of the medialmost extension of the canal clearly

388   shows that the growth center is much distal (at about 70% of the bone length for both

389   samples) in the humerus, and much proximal (at about 30% for QM and 40% for MU) in the

390   femur. Growth is thus clearly not symmetrical in most taxa of our sample, being much more

391   intense proximally in the humerus and distally in the femur. This confirms previous

392   observations made on humans (e.g., Ollier, 1867) but also preliminary observations made on

393   fossil whales (Houssaye et al. 2015). However, a proximal growth center has been observed in

394   the humerus of turtles (Nakajima et al., 2014). If our result appears thus rather general in

395   mammals, in cannot be generalized outside of Mammalia and further studies are required to

396   investigate this question in other amniotes.

397   Canals are generally straight with only a few exceptions occurring. The relative

398   extension of these canals along the diaphyseal cortex (H) is limited (<15% L with average

399   values between 3 and 9% L). However this corresponds to minimal estimates since the

400   position of the growth center cannot be ascertained precisely. Moreover, a few taxa display

401   high values (e.g. 26% L in *Choeropsis* humerus, 15% in *Rangifer* and *Lontra felina* femur).

402   Our study also clearly reveals that horizontal or subhorizontal canals are rare. The nutrient

403   foramen thus does not indicate the location of the growth center. It has been assumed that the

404   nutrient foramen was originally located at the level of the growth center but that an

405   asymmetrical growth could engender the foramen to move proximally or distally, towards the

406   faster growing end (Hughes, 1952; Henderson, 1978). Our results confirm that the canals are

407   essentially oriented towards the faster growing end.

408   There is a high variation in the orientation of the canals in the bone within mammals.

409   However, it was interesting to note preferential or absent orientations in the mustelid sample,

410   that probably reflect morphological constraints during development that would be specific to

411   these taxa, and thus that would imply stronger constraints at smaller taxonomical scales.

412   Similarly, the much higher canal obliquity and cortical height in mustelid femora than in the

413   other samples could also reflect specific developmental constraints. As a consequence, if the

414   biological information could be flooded in a large sample of diverse taxa, more specific

415   patterns might be revealed at a smaller taxonomic scale.

416

417

429

References

431

432   **Ahn DC** (2013) Anatomical study on the diaphyseal nutrient foramen of the femur and tibia

433   of the german shepherd dog. *J Vet Med Sci* 75, 803–808.

434   **Artec 3D** (2018) Artec Studio Professional. Artec 3D.

435   **Bisgard JD, Bisgard M** (1935) Longitudinal growth of long bones. *Arch Surg* 31, 568–578.

436   **Blomberg SP, Garland T, Ives AR** (2003) Testing for phylogenetic signal in comparative

437   data: behavioral traits are more labile. *Evolution* 57, 717–745.

438   **Botton-Divet L, Cornette R, Fabre AC, Herrel A, Houssaye A** (2016) Morphological

439   analysis of long bones in semi-aquatic mustelids and their terrestrial relatives. *Integr Comp*

440   *Biol* 56, 1298–1309.

441   **Campos FF, Pellico LG, Alias MG, Fernandez-Valencia R** (1987) A study of the nutrient

442   foramina in human long bones. *Surg Radiol Anat* 9, 251–255.

443   **Carter DR, Beaupré GS** (2007) Skeletal function and form: mechanobiology of skeletal

444   development, aging, and regeneration. Cambridge University Press.

445   **David CC, Jacobs DJ** (2014) Principal component analysis: a method for determining the

446   essential dynamics of proteins, in: protein dynamics, methods in molecular biology. Humana

447   press, Totowa, NJ, pp. 193–226.

448   **Digby KH** (1916) The measurement of diaphysial growth in proximal and distal directions. *J*

449   *Anat Physiol* 50, 187–188.

450   **Gümüsburun E, Yücel F, Ozkan Y, Akgün Z** (1994) A study of the nutrient foramina of

451   lower limb long bones. *Surg Radiol Anat* 16, 409–412.

452   **Haines RW** (1969) Epiphyses and sesamoids. Biology of the Reptilia 1, 81–115.

453   **Henderson R** (1978) The position of the nutrient foramen in the growing tibia and femur of

454   the rat. *J Anat* 125, 593–599.

455   **Houssaye A, Botton-Divet L** (2018) From land to water: evolutionary changes in long bone

456   microanatomy of otters (Mammalia: Mustelidae). *Biol J Linn Soc* 125, 240–249.

457   **Houssaye A, Tafforeau P, de Muizon C, Gingerich PD** (2015) Transition of Eocene whales

458   from land to sea: evidence from bone microstructure. *PloS One* 10, e0118409.

459   **Houssaye A, Taverne M, Cornette R** (2018) 3D quantitative comparative analysis of long

460   bone diaphysis variations in microanatomy and cross-sectional geometry. *J Anat* 232, 836–

461   849.

462   **Hughes H** (1952) The factors determining the direction of the canal for the nutrient artery in

463   the long bones of mammals and birds. *Cells Tissues Organs* 15, 261–280.

464   **Kizilkanat E, Boyan N, Ozsahin ET, Soames R, Oguz O** (2007) Location, number and

465   clinical significance of nutrient foramina in human long bones. *Ann Anat* 189, 87–95.

466   **Longia G, Ajmani M, Saxena S, Thomas R** (1980) Study of diaphyseal nutrient foramina in

467   human long bones. *Cells Tissues Organs* 107, 399–406.

468   **Meredith RW, Janečka JE, Gatesy J, Ryder OA, Fisher CA, Teeling EC, Goodbla A,**

469   **Eizirik E, Simão TL, Stadler T** (2011) Impacts of the Cretaceous terrestrial revolution and

470   KPg extinction on mammal diversification. *Science* 334, 521–524.

471   **Mysorekar V** (1967) Diaphysial nutrient foramina in human long bones. *J Anat* 101, 813–

472   822.

473   **Nagel A** (1993) The clinical significance of the nutrient artery. *Orthopaedic rev* 22, 557–561.

474   **Nakajima Y, Hirayama R, Endo H** (2014) Turtle humeral microanatomy and its

475   relationship to lifestyle. *Biol J Linn Soc* 112, 719–734.

476   **Ollier L** (1867) Traité expérimental et clinique de la régénération des os et de la production

477   artificielle du tissu osseux. V. Masson et fils, 548p.

478   **Patake S, Mysorekar V** (1977) Diaphysial nutrient foramina in human metacarpals and

479   metatarsals. *J Anat* 124, 299–304.

480   **Payton CG** (1932) The growth in length of the long bones in the madder-fed pig. *J Anat* 66,

481   414-425.

482   **Pereira G, Lopes P, Santos A, Silveira F** (2011) Nutrient foramina in the upper and lower

483   limb long bones: morphometric study in bones of Southern Brazilian adults. *Int J Morphol* 29,

484   514–20.

485   **R Development Core Team** (2014) R: a language and environment for statistical computing.

486   Vienna: R Foundation for Statistical Computing. Available at http://www.R-project.org/.

487   **Ross M, Pawlina W** (2011) Histology: a Text and Atlas, Alphen aan den Rijn, Netherlands.

488   **Sendemir E, Cimen A** (1991) Nutrient foramina in the shafts of lower limb long bones:

489   situation and number. *Surg Radiol Anat* 13, 105–108.

490   **Seymour RS, Smith SL, White CR, Henderson DM, Schwarz-Wings D** (2011) Blood flow

491   to long bones indicates activity metabolism in mammals, reptiles and dinosaurs. *Proc R Soc*

492   *B: Biol Sci* 279, 451–456.

493   **Sim JH, Ahn D** (2014) Anatomy of the diaphyseal nutrient foramen in the long bones of the

494   pectoral limb of German Shepherds. *Korean J Vet Res* 54, 179–184.

495   **Slater GJ, Harmon LJ, Alfaro ME** (2012) Integrating fossils with molecular phylogenies

496   improves inference of trait evolution. *Evolution* 66, 3931–3944.

497

498

499   The data that support the findings will be available in the 3Dthèque of the MNHN -

500   https://3dtheque.mnhn.fr/- under request.

501

502   **Tables**

503

504   Table 1. List of the material analyzed in this study. QM: dataset of the various quadrupedal

505   mammal species; MU: dataset of the mustelids; H: humerus; F: femur. Abb: abbreviations,

506   later used in figures. Institutional abbreviations: MNHN: Museum National d'Histoire

507   Naturelle, Paris, France; SMNS: Staatliches Museum für Naturkunde Stuttgart, Germany;

508   STIPB, Steinmann-Institut, Universität Bonn, Germany; UAM: the University of Alaska

509   Museum, Fairbanks, USA; UFGK, Ur- und Frühgeschichte Köln, Köln, Germany; ZFMK,

510   Zoologisches Forschungsmuseum Alexander Koenig, Bonn, Germany.

511

	Taxon	Abb.	Dataset	Collection Nb.	Bone
Caviidae	*Cavia porcellus*	Cp	QM	STIPB Unnumbered	F
Sciuridae	*Marmota marmota*	Mma	QM	STIPB Unnumbered	H,F
Tupaiidae	*Tupaia belangeri*	Tb	QM	STIPB Unnumbered	H,F
Erinaceidae	*Erinaceus europaeus*	Ee	QM	STIPB Unnumbered	H,F
Talpidae	*Talpa europaea*	Te	QM	STIPB Unnumbered	H,F
Suidae	*Sus scrofa*	Ss	QM	STIPB M56	H,F
Hippopotamidae	*Choeropsis liberiensis*	Cl	QM	ZFMK 65 570	H,F
Cervidae	*Rangifer tarandus*	Rt	QM	STIPB M47	H,F
Cervidae	*Dama dama*	Dd	QM	STIPB M1	H
Bovidae	*Rupicapra rupicapra*	Rr	QM	STIPB M1639	H,F
Felidae	*Felis silvestris*	Fs	QM	UFGK Unnumbered	H,F
Canidae	*Vulpes vulpes*	Vv	QM	STIPB M12	H,F
Mustelidae	*Meles meles*	Mme	QM MU	STIPB M4002	H,F
Mustelidae	*Martes martes*	Mm	QM MU	STIPB Unnumbered	H,F
Mustelidae	*Mustela putorius*	Mp	QM MU	STIPB Unnumbered	H,F
Mustelidae			MU	MNHN 1997-440	H,F
Mustelidae			MU	MNHN 2004-639	H,F
Mustelidae	*Mustela eversmannii*	Me	MU	MNHN 2005-668	H,F,F
Mustelidae	*Neovison vison*	Ne	MU	MNHN 1958-165	H,F,F
Mustelidae	*Pteronura brasiliensis*	Pb	MU	MNHN A1918	H,F
Mustelidae			MU	SMNS 1300	H,F,F

Mustelidae	*Lontra felina*	Lf	MU	MNHN 1884-874	H,F
Mustelidae			MU	MNHN 1995-185	H,F,F
Mustelidae	*Lontra canadensis*	Lc	MU	UAM 53927	H,F
Mustelidae			MU	UAM 67696	H,F
Mustelidae	*Lutra lutra*	Ll	MU	MNHN 1996-2466	H,F
Mustelidae	*Enhydra lutris*	El	MU	MNHN 1935-124	H,F
Mustelidae			MU	MNHN A12503	H,F

512
513
514

Table 2. P-values from the Anovas on the link between the number of nutrient canals (NNC) and the various continuous characters (for the datasets including all canals). Abbreviations as in Material and Methods. In bold when significant at 5%.

518

D/P	R	FI	CDr	CDEr	CO	H	L	LR
H QM	p=0.39	p=0.47	**p<0.001**	**p=0.008**	**p=0.004**	p=0.68	p=0.08	**p<0.001**
F QM	p=0.77	p=0.98	**p=0.02**	p=0.70	p=0.07	p=0.20	p=0.31	**p=0.01**
H MU	**p=0.02**	p=0.44	**p=0.04**	p=0.10	p=0.85	p=0.67	**p=0.009**	**p=0.03**
F MU	p=0.14	p=0.43	**p=0.003**	**p=0.02**	p=0.83	p=0.27	p=0.49	**p=0.04**

519
520

Table. 3. K-statistics with the associated p-values for the continuous parameters. In bold when significant at 5%.

Dataset/Parameter	FI	CD	CDE	CO	H	R
Humerus QM	K=0.44 p=0.22	K=0.65 p=0.08	K=0.45 p=0.15	K=0.32 p=0.80	K=0.46 p=0.32	**K=1.40 p<0.001**
Femur QM	K=0.46 p=0.24	K=0.42 p=0.47	K=0.40 p=0.43	K=0.41 p=0.66	K=0.36 p=0.80	K=0.48 p=0.23
Humerus MU	**K=1.01 p=0.049**	**K=1.34 p=0.003**	**K=1.41 p=0.002**	K=0.73 p=0.08	K=0.73 p=0.11	K=0.74 p=0.10
Femur MU	K=0.81 p=0.07	K=0.84 p=0.10	**K=1.46 p=0.03**	K=0.69 p=0.10	**K=1.57 p=0.005**	K=0.73 p=0.13

523
524

Table 4. Results of the linear regressions performed on the datasets (with R as a size estimate). AC: all canals; I: averaged by individual; In bold when significant at 5%.

Dataset/Parameter	FI	CD	CDE	CDsum	CDEsum	CO	H
Humerus QM AC	R=-0.21 p=0.37	**R=0.79 p<0.001**	**R=0.59 p=0.01**	-	-	R=0.20 p=0.40	R=0.35 p=0.13
Femur QM AC	R=0.04 p=0.86	**R=0.82 p<0.001**	**R=0.93 p<0.001**	-	-	R=-0.26 p=0.22	R=0.16 p=0.47
Humerus MU AC	R=0.09 p=0.68	**R=0.86 p<0.001**	**R=0.65 p<0.001**	-	-	R=-0.10 p=0.67	R=-0.01 p=0.98
Femur MU AC	R=0.24 p=0.22	**R=0.56 p<0.001**	**R=0.51 p=0.005**	-	-	R=-0.03 p=0.88	R=0.20 p=0.30
Humerus QM I	R=-0.28 p=0.34	**R=0.80 p<0.001**	**R=0.63 p=0.02**	**R=0.90 p<0.001**	**R=0.85 p<0.001**	R=-0.01 p=0.98	R=0.36 p=0.21
Femur QM I	R=0.23 p=0.43	**R=0.83 p<0.001**	**R=0.94 p<0.001**	**R=0.92 p<0.001**	**R=0.85 p<0.001**	R=-0.08 p=0.79	R=0.48 p=0.07
Humerus MU I	R=0.22 p=0.43	**R=0.88 p<0.001**	**R=0.59 p=0.02**	**R=0.85 p<0.001**	**R=0.53 p=0.03**	R=-0.12 p=0.66	R=-0.10 p=0.71
Femur MU I	R=0.35 p=0.13	**R=0.58 p=0.01**	**R=0.46 p=0.04**	**R=0.86 p<0.001**	**R=0.70 p<0.001**	R=-0.01 p=0.95	R=0.33 p=0.15

527

528

Table 5. Results of the linear regressions performed on the datasets with L and LR. In bold when significant at 5%. D/P: Dataset/Parameter; Var: variable; other abbreviations as in Table 3.

D/P	FI		CDr		CDEr		CDrsum		CDErsum		CO		H	
Var	L	LR	L	LR	L	LR	L	LR	L	LR	L	LR	L	LR
HQMAC	R=-0.20 p=0.40	R=0.15 p=0.53	R=-0.16 p=0.50	**R=0.72 p<0.001**	R=-0.06 p=0.79	**R=0.45 p=0.047**	-	-	-	-	R=0.41 p=0.08	**R=0.63 p=0.003**	R=0.36 p=0.12	R=0.08 p=0.73
FQMAC	R=0.06 p=0.79	R=-0.16 p=0.46	R=-0.08 p=0.71	**R=0.44 p=0.03**	R=-0.09 p=0.69	R=0.08 p=0.70	-	-	-	-	R=-0.12 p=0.56	R=0.26 p=0.22	R=0.27 p=0.20	R=0.06 p=0.78
HMUAC	R=0.19 p=0.40	R=0.20 p=0.37	R=0.10 p=0.65	R=0.37 p=0.09	R=0.07 p=0.75	R=0.31 p=0.17	-	-	-	-	R=-0.05 p=0.83	R=0.13 p=0.56	R=-0.07 p=0.75	R=-0.21 p=0.36
FMUAC	R=-0.03 p=0.89	**R=-0.60 p<0.001**	R=-0.32 p=0.09	**R=0.56 p=0.002**	R=-0.21 p=0.28	**R=0.60 p<0.001**	-	-	-	-	R=-0.14 p=0.47	R=-0.28 p=0.14	R=-0.14 p=0.47	**R=-0.70 p<0.001**
HQMI	R=-0.28 p=0.33	R=0.23 p=0.43	R=-0.46 p=0.10	**R=0.64 p=0.01**	R=-0.19 p=0.52	R=0.31 p=0.27	**R=-0.56 p=0.04**	R=0.21 p=0.48	R=-0.23 p=0.44	R=0.00 p=1.00	R=0.18 p=0.55	R=0.46 p=0.10	R=0.39 p=0.17	R=-0.02 p=0.95
FQMI	R=0.25 p=0.39	R=-0.24 p=0.40	R=-0.12 p=0.67	R=0.39 p=0.17	R=-0.12 p=0.68	R=0.06 p=0.84	R=-0.23 p=0.42	R=-0.06 p=0.84	R=-0.19 p=0.52	R=-0.32 p=0.27	R=0.07 p=0.82	R=0.23 p=0.43	**R=0.57 p=0.03**	R=-0.15 p=0.61

HMUI	R=0.34 p=0.20	R=0.24 p=0.37	R=0.09 p=0.75	**R=0.55 p=0.03**	R=0.04 p=0.89	R=0.46 p=0.07	R=0.09 p=0.75	**R=0.55 p=0.03**	R=-0.39 p=0.14	**R=0.72 p=0.001**	R=-0.05 p=0.84	R=0.19 p=0.47	R=-0.18 p=0.50	R=-0.23 p=0.40
FMUI	R=0.04 p=0.85	**R=-0.71 p<0.001**	R=-0.38 p=0.10	**R=0.52 p=0.02**	R=-0.3 p=0.20	**R=0.56 p=0.01**	R=-0.23 p=0.32	**R=0.45 p=0.047**	R=-0.12 p=0.62	**R=0.55 p=0.01**	R=-0.14 p=0.56	R=-0.26 p=0.26	R=-0.05 p=0.84	**R=-0.82 p<0.001**

532

533

534 **Figure legends**

535

536 Figure 1. 3D reconstructions showing how the foraminal index (FI) was calculated for the

537 nutrient canal (in purple), based on bone length (L) and the distance between the proximal

538 extremity and the nutrient foramen (d). A- Humerus of *Rangifer tarandus* STIPB M47. B-

539 Femur of *Mustela eversmannii* MNHN 2005-668.

540 Figure 2. 3D reconstructions showing the number and orientation of the nutrient canals. A-

541 Two canals distalo-proximally oriented in the humerus of *Dama dama* STIPB M1; B- four

542 horizontal canals in the humerus of *Talpa europaea* STIPB Unnumbered; C- two canals

543 proximo-distally oriented and in the femur of *Lontra felina* MNHN 1884-874; and D- a single

544 canal proximo-distally oriented in the femur of *Felis silvestris* UFGK Unnumbered.

545 Figure 3. Boxplots illustrating the variation of the various parameters pending on the samples.

546 FI: foraminal index; CDr: relative canal diameter; CDEr: relative canal diameter at the outer

547 extremity; CO: canal obliquity; H: canal cortical height; R: bone mean diaphyseal radius.

548 Figure 4. Distribution of the specimens in the morphospace and contribution of the various

549 parameters along the two first axes of the humerus PCA for the quadrupedal mammal (all

550 canals) sample. Abbreviations as in Fig. 3 and Table 1.

551 Figure 5. Distribution of the specimens in the morphospace and contribution of the various

552 parameters along the two first axes of the femur PCA for the quadrupedal mammal sample.

553 A- all canals; B- all specimens. Abbreviations as in Fig. 3 and Table 1.

554 Figure 6. Distribution of the mustelid specimens in the morphospace and contribution of the

555 various parameters along the two first axes of the humerus PCA. A- all canals; B- all

556 specimens. Yellow: Mustelinae; Blue: Lutrinae. Abbreviations as in Fig. 3 and Table 1.

557 Figure 7. Distribution of the mustelid specimens in the morphospace and contribution of the

558 various parameters along the two first axes of the femur PCA on all canals. Yellow:

559 Mustelinae; Blue: Lutrinae. Abbreviations as in Fig. 3 and Table 1.

560

561 **Supporting Information**

562 **Fig. S1.** Phylogeny including the species used in this study. A- The quadrupedal mammal

563 (QM) sample, based on Meredith et al. (2011); B- The Mustelidae (Mu) sample, based on

564 Slater, Harmon & Alfaro (2012).

565

566 **Table S1.** Values of the parameters for the humerus QM dataset. Med: medial; Lat: lateral;
567 Ant: anterior; Post: posterior; DP: distalo-proximal; H: horizontal; PD: proximo-distal; S:
568 straight; A: angled.

Taxon	Direction	Orientation	Shape	NNC	R (mm)	FI	CD (mm)	CDE (mm)	CO (°C)	H
Marmota	Med	DP	S	1	3.93	0.67	0.64	1.40	61.7	0.02
Tupaia	Lat	DP	S	1	1.70	0.75	0.21	0.25	37.6	0.01
Erinaceus	Post	DP	S	1	2.53	0.53	0.19	0.20	71.8	0.09
Talpa	Post	DP	S	4	2.35	0.60	0.10	0.17	28.0	0.04
	Post	DP	S	4	2.35	0.60	0.04	0.04	27.6	0.04
	Post	H	S	4	2.35	0.62	0.06	0.11	3.0	0.01
	Ant-lat	H	S	4	2.35	0.68	0.09	0.09	3.1	0.03
Sus	Post	DP	S	1	12.49	0.57	0.91	2.51	60.5	0.09
Choeropsis	Post	DP	S	2	16.32	0.34	1.02	1.67	69.5	0.26
	Med	H	S	2	16.32	0.75	0.81	0.47	13.1	0.01
Rangifer	Ant	DP	A	1	14.06	0.74	0.95	2.63	34.0	0.01
Dama	Post	DP	S	2	13.42	0.61	0.65	0.98	63.0	0.05
	Ant-med	DP	S	2	13.42	0.69	0.31	0.46	50.0	0.03
Rupicapra	Lat	DP	S	2	8.76	0.66	0.43	0.28	70.8	0.06
	Post	DP	S	2	8.76	0.43	0.56	0.53	80.1	0.11
Felis	Med	DP	S	1	4.90	0.67	0.51	0.64	64.7	0.06
Vulpes	Post	DP	S	1	5.19	0.52	0.44	0.46	80.8	0.13
Meles	Med	PD	A	1	7.02	0.73	0.77	0.54	49.2	0.03
Martes	Med	DP	A	1	2.72	0.76	0.44	0.75	33.7	0.01
Mustela	Ant	PD	A	1	2.43	0.76	0.30	0.43	57.8	0.03

569

570

571 **Table S2.** Values of the parameters for the femur QM dataset. Abbreviations as in Table S1.

Taxon	Direction	Orientation	Shape	NNC	R (mm)	FI	CD (mm)	CDE (mm)	CO (°C)	H
Cavia	Post-med	PD	S	1	2.74	0.30	0.23	0.39	52.9	0.05
Marmota	Med	PD	S	1	4.00	0.33	0.35	0.87	70.4	0.06
Tupaia	Med	PD	S	1	1.27	0.29	0.23	0.23	63.9	0.02
Erinaceus	Ant-med	PD	S	4	2.32	0.38	0.26	0.73	51.9	0.06
	Med-ant	PD	S	4	2.32	0.32	0.12	0.19	44.8	0.05
	Ant	PD	S	4	2.32	0.30	0.11	0.07	36.8	0.02
	Ant	DP	S	4	2.32	0.26	0.09	0.08	24.0	0.01
Talpa	Lat	PD	S	3	1.13	0.53	0.06	0.21	64.2	0.05
	Med-post	PD	S	3	1.13	0.54	0.08	0.14	68.4	0.04
	Ant	PD	S	3	1.13	0.52	0.06	0.09	70.0	0.03
Sus	Post	PD	S	1	11.37	0.56	0.66	1.28	80.7	0.08
Choeropsis	Med-ant	PD	S	3	17.84	0.42	0.72	1.72	47.1	0.04
	Ant	PD	S	3	17.84	0.36	1.28	2.16	21.0	0.01

	Ant-med	H	S	3	17.84	0.33	0.81	2.47	4.1	0.00
Rangifer	Ant	DP	A	1	14.94	0.36	1.96	2.44	61.4	0.15
Rupicapra	Ant	PD	S	2	8.49	0.24	0.79	1.18	36.6	0.01
	Post	DP	S	2	8.49	0.61	0.51	0.41	88.3	0.13
Felis	Post	PD	S	1	4.78	0.41	0.36	0.39	70.0	0.04
Vulpes	Post	DP	S	1	5.45	0.30	0.56	0.60	62.5	0.03
Meles	Post	PD	S	2	6.94	0.52	0.37	0.67	68.1	0.08
	Med	PD	S	2	6.94	0.41	0.32	0.60	41.0	0.02
Martes	Post-lat	PD	S	2	2.91	0.37	0.36	0.61	46.3	0.04
	Post-lat	PD	S	2	2.91	0.37	0.18	0.41	44.2	0.03
Mustela	Post	PD-H	S	1	2.65	0.34	0.21	0.14	18.8	0.01

572

573

574 **Table S3.** Values of the parameters for the humerus MU dataset. Abbreviations as in Table
575 S1. SE: serpentiform.

Taxon	Direction	Orientation	Shape	NNC	R (mm)	FI	CD (mm)	CDE (mm)	CO (°C)	H
Meles	Med	PD	A	1	7.02	0.73	0.77	0.54	49.2	0.03
Martes	Med	DP	A	1	2.72	0.76	0.44	0.75	33.7	0.01
Mustela putorius	Ant	PD	A	1	2.43	0.76	0.30	0.43	57.8	0.03
	Post	DP	S	3	0.96	0.59	0.09	0.09	73.6	0.08
	Ant	DP	S	3	0.96	0.73	0.08	0.13	31.1	0.01
	Ant	H	S	3	0.96	0.72	0.04	0.03	10.7	0.01
	Post	DP	A	1	1.22	0.62	0.18	0.13	55.6	0.05
Mustela eversmanni	Ant	PD	A	2	1.15	0.75	0.14	0.23	25.4	0.02
	Ant	DP	S	2	1.15	0.71	0.10	0.13	60.6	0.02
Neovison	Ant	DP	S	2	1.15	0.69	0.11	0.14	45.8	0.03
	Ant	DP	S	2	1.15	0.71	0.15	0.16	34.8	0.01
Pteronura	Ant	PD	A	1	3.36	0.75	0.25	0.31	17.1	0.02
	Ant	DP	A	1	3.18	0.71	0.23	0.27	47.5	0.01
Lontra felina	Ant	PD	SE	1	2.04	0.69	0.23	0.20	53.1	0.06
	Med	DP	S	1	2.58	0.62	0.22	0.49	41.4	0.05
Lontra canadensis	Ant-med	DP	S	1	3.03	0.65	0.39	0.40	61.6	0.04
	Med-post	DP	S	2	2.81	0.46	0.09	0.09	49.6	0.14
	Med	DP	S	2	2.81	0.7	0.27	0.33	48.1	0.03
Lutra	Med	H	S	1	2.78	0.73	0.28	0.45	7.9	0.00
Enhydra	Ant	DP	S	1	3.67	0.72	0.34	0.63	22.5	0.02
	Ant	H	A	2	3.92	0.72	0.20	0.38	3.7	0.02
	Ant	DP	S	2	3.92	0.65	0.33	0.37	48.0	0.04

576

577

578 **Table S4.** Values of the parameters for the femur MU dataset. Abbreviations as in Table S1.

| Taxon	Direction	Orientation	Shape	NNC	R (mm)	FI	CD (mm)	CDE (mm)	CO (°C)	H
Meles	Post	PD	S	2	6.94	0.52	0.37	0.67	68.1	0.08
	Med	PD	S	2	6.94	0.41	0.32	0.60	41.0	0.02
Martes	Post-lat	PD	S	2	2.91	0.37	0.36	0.61	46.3	0.04
	Post-lat	PD	S	2	2.91	0.37	0.18	0.41	44.2	0.03
Mustela putorius	Post	PD-H	S	1	2.65	0.34	0.21	0.14	18.8	0.01
	Post-med	PD	S	1	1.23	0.36	0.29	0.42	21.3	0.01
	Post	PD	S	1	0.97	0.39	0.12	0.26	67.3	0.03
Mustela eversmanni	Post-lat	DP	S	2	1.10	0.33	0.12	0.17	19.2	0.01
	Post	PD	S	2	1.10	0.4	0.15	0.24	46.5	0.02
	Post	PD	S	1	1.12	0.4	0.26	0.49	66.3	0.03
Neovison	Post	PD	S	1	1.09	0.45	0.11	0.11	71.0	0.06
	Post	PD	S	1	1.11	0.47	0.09	0.11	75.2	0.08
Pteronura	Post	PD	S	1	2.83	0.48	0.32	0.32	67.5	0.09
	Post-med	PD	S	1	3.65	0.56	0.37	0.38	77.5	0.15
	Post	PD	S	1	3.3	0.56	0.31	0.32	76.2	0.15
Lontra felina	Post	PD	S	1	2.29	0.53	0.25	0.29	77.7	0.14
	Post	PD	S	1	2.28	0.48	0.22	0.54	69.0	0.12
	Post	PD	S	2	1.89	0.5	0.17	0.19	71.4	0.13
	Med	PD	S	2	1.89	0.55	0.05	0.04	77.7	0.17
Lontra canadensis	Post	PD	S	2	2.76	0.52	0.22	0.37	73.7	0.21
	Post	PD	S	2	2.76	0.45	0.18	0.15	60.4	0.07
	Post-med	PD	S	3	2.64	0.58	0.16	0.18	75.3	0.18
	Med	PD	S	3	2.64	0.54	0.16	0.18	75.0	0.14
	Post	PD	S	3	2.64	0.43	0.08	0.13	56.4	0.06
Lutra	Post	PD	S	1	2.66	0.45	0.24	0.27	69.6	0.09
Enhydra	Post-med	PD	S	2	4.42	0.42	0.40	0.46	67.8	0.12
	Post	PD	S	2	4.42	0.57	0.11	0.11	70.6	0.17
	Post	PD	S	2	4.48	0.58	0.30	0.31	54.4	0.21
	Med-post	PD	S	2	4.48	0.35	0.23	0.33	20.9	0.05

579
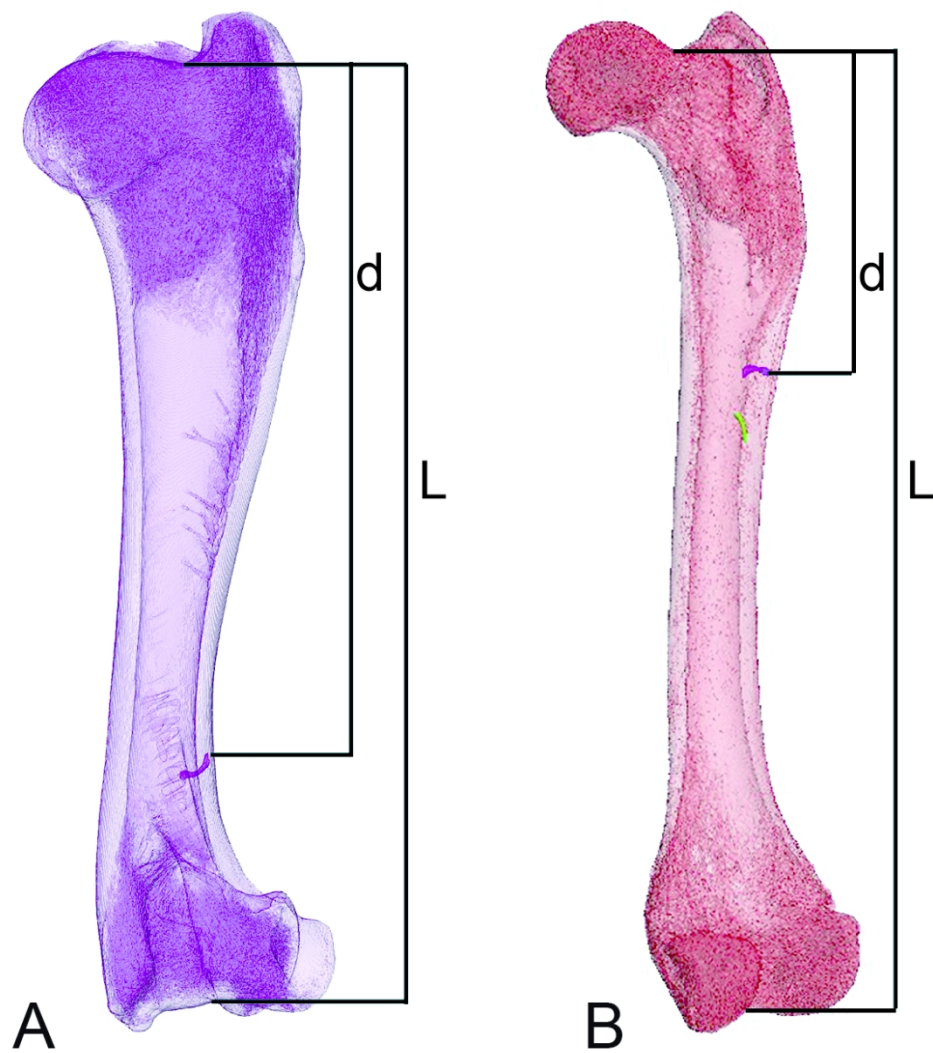
Figure 1. 3D reconstructions showing how the foraminal index (FI) was calculated for the nutrient canal (in purple), based on bone length (L) and the distance between the proximal extremity and the nutrient foramen (d). A- Humerus of Rangifer tarandus STIPB M47. B- Femur of Mustela eversmannii MNHN 2005-668.
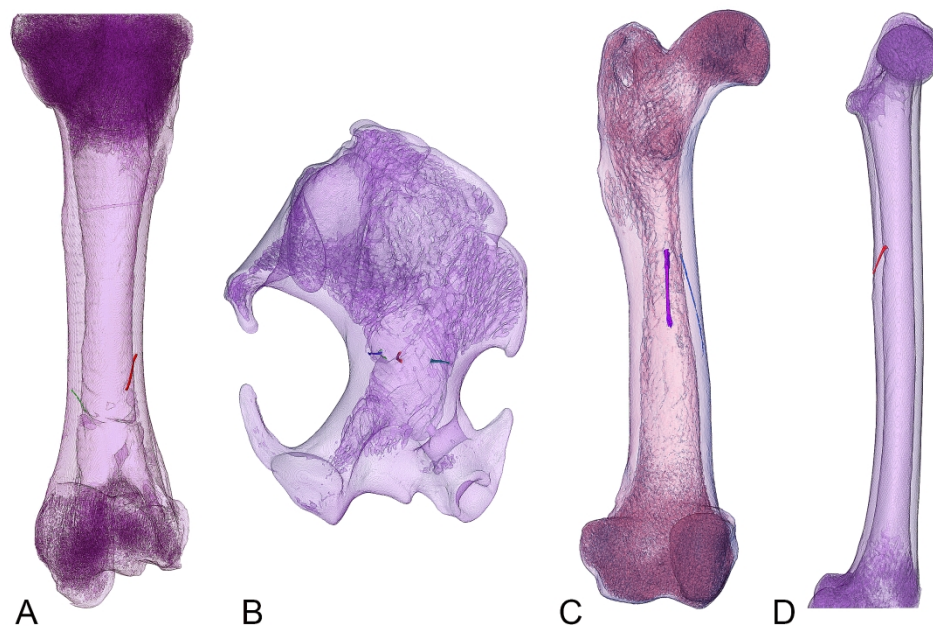
Figure 2. 3D reconstructions showing the number and orientation of the nutrient canals. A- Two canals distalo-proximally oriented in the humerus of Dama dama STIPB M1; B- four horizontal canals in the humerus of Talpa europaea STIPB Unnumbered; C- two canals proximo-distally oriented and in the femur of Lontra felina MNHN 1884-874; and D- a single canal proximo-distally oriented in the femur of Felis silvestris UFGK Unnumbered.
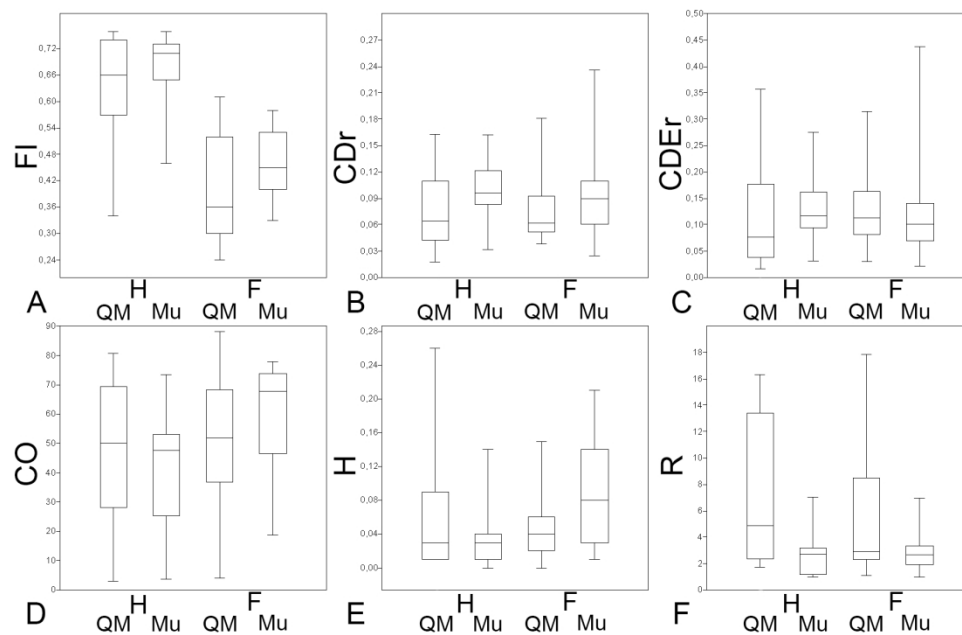
Figure 3. Boxplots illustrating the variation of the various parameters pending on the samples. FI: foraminal index; CDr: relative canal diameter; CDEr: relative canal diameter at the outer extremity; CO: canal obliquity; H: canal cortical height; R: bone mean diaphyseal radius.
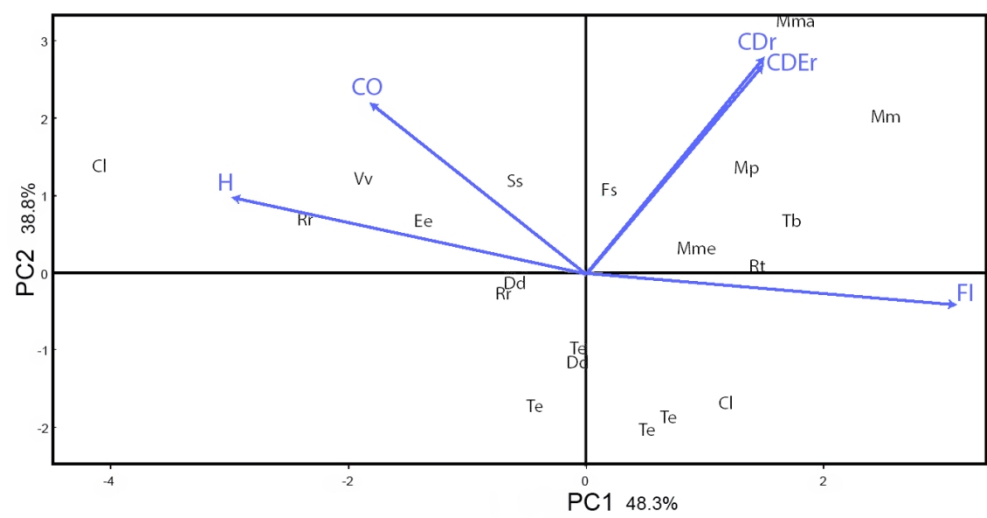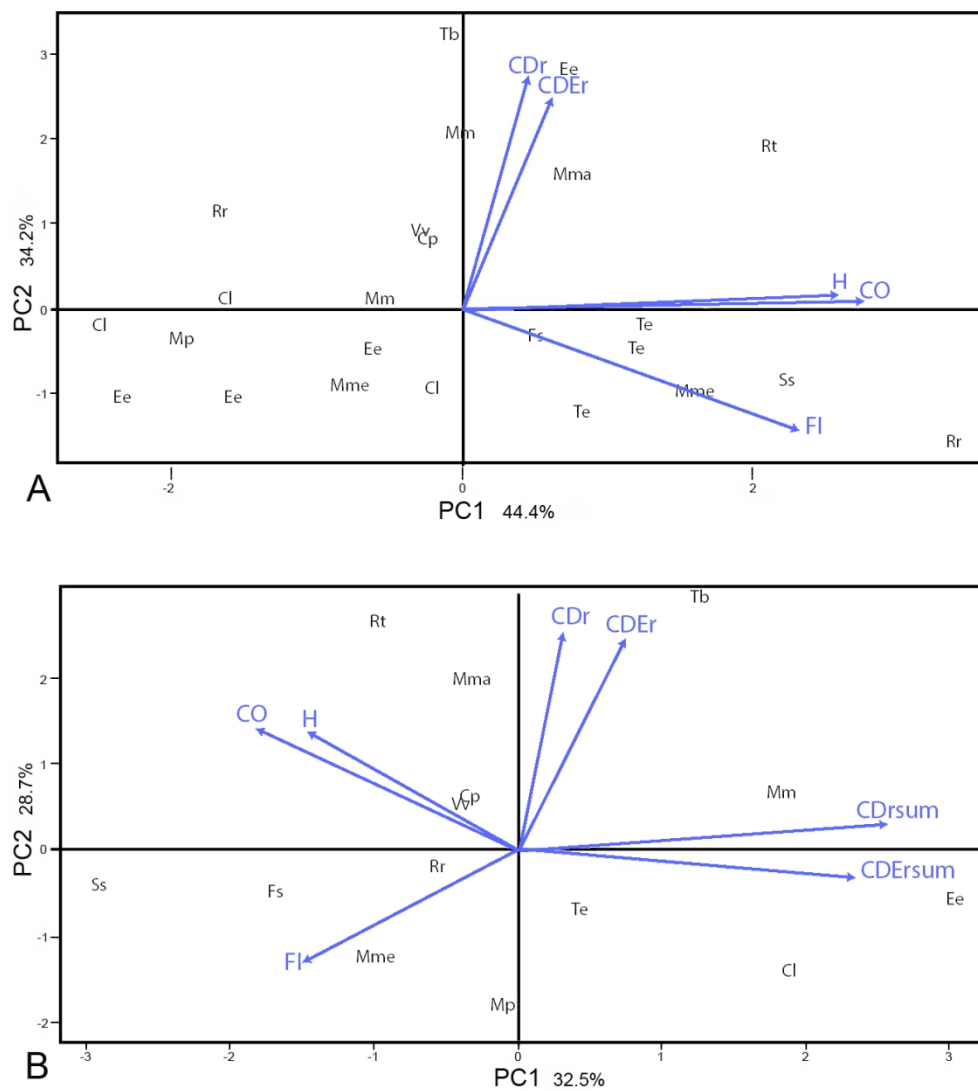
Figure 4. Distribution of the specimens in the morphospace and contribution of the various parameters along the two first axes of the humerus PCA for the quadrupedal mammal (all canals) sample. Abbreviations as in Fig. 3 and Table 1.

Figure 5. Distribution of the specimens in the morphospace and contribution of the various parameters along the two first axes of the femur PCA for the quadrupedal mammal sample. A- all canals; B- all specimens. Abbreviations as in Fig. 3 and Table 1.
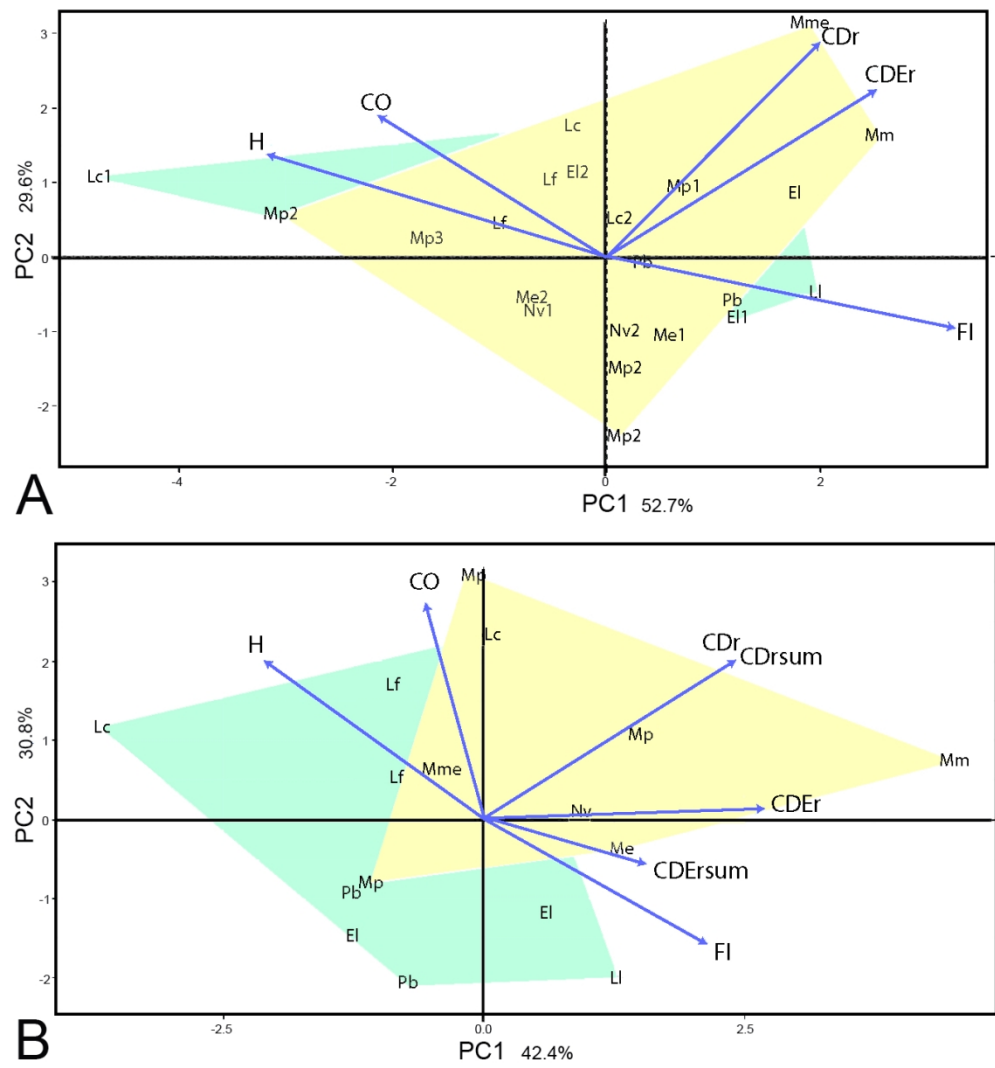
Figure 6. Distribution of the mustelid specimens in the morphospace and contribution of the various parameters along the two first axes of the humerus PCA. A- all canals; B- all specimens. Yellow: Mustelinae; Blue: Lutrinae. Abbreviations as in Fig. 3 and Table 1.
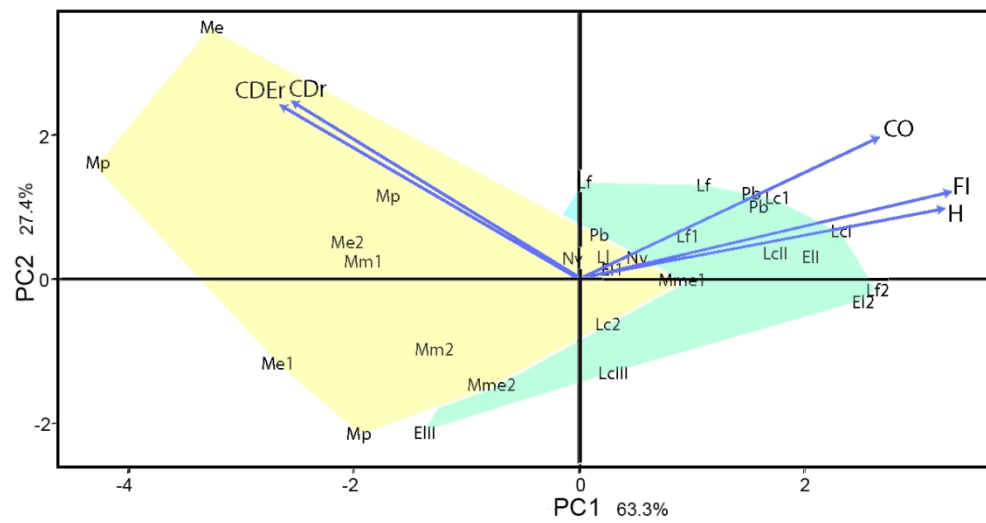
Figure 7. Distribution of the mustelid specimens in the morphospace and contribution of the various parameters along the two first axes of the femur PCA on all canals. Yellow: Mustelinae; Blue: Lutrinae. Abbreviations as in Fig. 3 and Table 1.

A

B